Particle Sampling in Supersonic Streams with a Thin-Walled Cylindrical Probe

L. J. Forney*
Georgia Institute of Technology, Atlanta, Georgia
and
W. K. McGregor†
Sverdrup Technology Inc., Arnold Air Force Station, Tennessee

The theoretical collection efficiency of a thin-walled cylindrical probe has been determined for nondiffusing particles of low concentration suspended in a supersonic stream. It is demonstrated that the probe capture efficiency is influenced by particle inertia, departures from Stokes drag, gas compressibility, and the probe ingestion rate. By defining an effective Stokes number in terms of the particle stopping distance downstream of the shock, which includes the effects of non-Stokesian drag and slip flow, and rescaling the Stokes number with the shock detachment distance, the reduced probe collection efficiency is shown to be correlated with a single universal curve. This similarity parameter should be useful in attempts to correlate the particle deposition for any geometry in a supersonic stream.

Nomenclature

A_p = cross-sectional area of particle, $\pi/4\ d_p^2$ (cm^2)
c = speed of sound (cm/s)
C_D = particle drag coefficient
D = probe diameter (cm)
d_p = particle diameter (cm)
E = probe collection efficiency, r_p^{+2}
E_p = reduced probe collection efficiency
f = probe mass fraction ingested, r_g^{+2}
Kn = particle Knudsen number
m_p = particle mass, $\pi d_p^3 \rho_p/6$ (gm)
M = freestream Mach number
r = radial coordinate (cm)
r_g = starting coordinate of limiting gas streamline (cm)
r_p = starting coordinate of limiting particle trajectory (cm)
R = probe radius (cm)
Re = local particle Reynolds number
Rep = particle Reynolds number
R_g = gas constant (cm^2/s^2-K)
T = gas temperature (K)
t = time (s)
u = particle velocity in x direction (cm/s)
u^+ = normalized particle velocity in x direction (u/v_1)
v = particle velocity in r direction (cm/s)
v^+ = normalized particle velocity in r direction (v/v_1)
v_1 = freestream gas velocity (cm/s)
ν = particle velocity vector (cm/s)
ν^+ = normalized particle velocity vector (ν/v_1)
ν_f = gas velocity vector (cm/s)
ν_f^+ = normalized gas velocity vector (ν_f/v_1)
x = axial coordinate (cm)
α = ratio of static-to-stagnation pressure inside probe
δ = shock detachment distance (cm)
γ = ratio of specific heats
μ = gas viscosity (gm/cm-s)
Φ_c = Cunningham slip correction factor
Φ_r = non-Stokesian correction factor
Φ_s = ratio of probe radius-to-shock detachment distance
ρ = gas density (gm/cm^3)
ρ_p = particle density (gm/cm^3)
Ψ = Stokes number
Ψ_c = particle impaction parameter, $\Psi\Phi_c$
Ψ_r = particle impaction parameter, $\Psi\Phi_c\Phi_r$
Ψ_f = particle impaction parameter, $\Psi\Phi_c\Phi_r\Phi_s$
θ = normalized time, $v_1 t/R$

Subscripts

01 = stagnation conditions upstream of shock
02 = stagnation conditions downstream of shock
f = gas velocity

Received Nov. 19, 1985; revision received Jan. 19, 1987.

*Associate Professor, School of Chemical Engineering.
†Senior Scientist.

I. Introduction

LIQUID and solid particles are formed in combustion processes. Initially, small submicron particles are formed by the condensation of super-saturated vapor, that may coagulate into larger liquid or solid particles. The knowledge of the size distribution and chemical composition of combustion-produced particles is important from the standpoint of system performance, and reliable measurement techniques are necessary to evaluate these particle parameters.

Large concentrations of particles or their incandescence (e.g., conditions typical of solid propellant rocket exhausts) may preclude the use of nonintrusive optical methods to determine particle size distributions. In these cases, the insertion of a particle probe directly into the supersonic particle-laden stream is necessary to extract a representative sample. Problems, however, are encountered when attempting to sample particles from the high-speed exhaust plumes of solid propellant rocket motors, jet engines, and some wind tunnels.

Sampling problems result from the complex gas flowfield that exists either external or internal to the probe, depending upon the design. The collection of particles from a supersonic gas stream requires that they be decelerated from supersonic to subsonic velocities. A supersonic probe can thus be classified in terms of how the gas flow is decelerated from supersonic to subsonic velocities as either an external

shock or a shock-swallowing design. In either case, particle discrimination can result from gas streamline curvature outside the probe (particle inertia), losses on internal walls (particle deposition), or droplet and agglomerate breakup (large-particle Weber number).

Probe designs for use in intrusive particle extraction within the exhaust plumes of solid propellant rocket motors must be of rugged construction to withstand the high velocity and temperature environment. The dimension of test facilities may prohibit the use of short sample lines. Thus, isokinetic sampling may be difficult to achieve, and a condition of "choked flow" may exist in the sample probe. Intrusive sampling from a supersonic stream under these conditions produces a detached shock in front of the particle collection probe. This external shock front creates some curvature in the gas streamlines near the sampling probe inlet, and a size-dependent preferential withdrawal of particles may take place.[1]

Alternative probe designs that swallow the shock subject the particles to either an under- or overexpanded supersonic jet located at a sudden enlargement in the internal probe diameter downstream from a supersonic inlet. Gas separation, recirculation, and turbulence that result from these complex internal probe geometries lead to significant wall losses. These wall losses may be reduced by injecting a clean supplementary gas into the probe. However, the injected gas temperature is normally significantly lower than the stagnation temperature of the particle-laden supersonic freestream, which can lead to an order of magnitude increase in the particle Weber number. Therefore, at present, the best alternative appears to be an external shock probe with an aerodynamically smooth internal wall that maintains the shock front close to the probe inlet and minimizes the particle Weber number or the likelihood of droplet or agglomerate breakup.

Figure 1 represents a schematic of an ideal thin-walled cylindrical probe aligned parallel to the freestream. Assuming that the Reynolds number based on the probe diameter is large so that the boundary layers are thin relative to the probe dimensions, the flowfield can be approximated as inviscid.[1,2] Inviscid solutions for the present geometry were obtained recently with a slight variant to MacCormack's time-dependent finite-difference method.[2] Reasonable agreement was demonstrated for the shock detachment distance, stagnation pressure loss, and inlet Mach number distributions predicted for a useful range of freestream Mach numbers and probe ingestion rates.

The purpose of the present paper is to document the results of the numerical computation of particle trajectories near the probe inlet. In particular, the effects of large-particle Knudsen and Reynolds numbers are demonstrated on the probe collection efficiency. The influence of the freestream Mach number and probe ingestion rate are also accounted for by rescaling the Stokes number with the shock detachment distance.

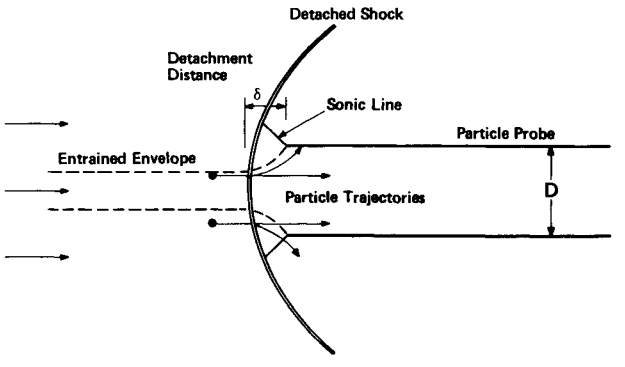

Fig. 1 Schematic of cylindrical particle probe in a supersonic stream.

II. Gas Flowfield

The numerical procedure used to determine the properties of the gas flowfield has been documented in a previous study.[2] In summary, imposing a reflection technique on the probe walls and tip and linear extrapolation on subsonic and supersonic outflows, MacCormack's iterative scheme with spacial smoothing on the first time step provided realistic solutions free of oscillations near the shock front. In particular, numerical computations of probe ingestion rates as a function of the ratio of static-to-stagnation pressure within the probe approached simple one-dimensional calculations for those probe boundary conditions that reduced shock curvature. These results are shown in Fig. 2.

The normalized gas density, two component velocities, and temperature were determined on the grid points of a 51×51 mesh, with 40 grid spaces across the probe radius for a variety of probe boundary conditions. The source code to determine the gas properties and the present code used to follow particles through the flowfield were executed on a

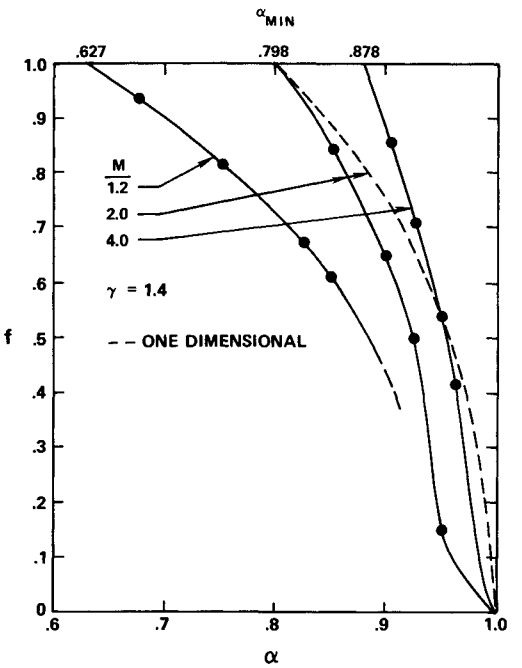

Fig. 2 Probe mass flowrate as a function of the static pressure at probe outlet. α is the ratio of static to stagnation pressure; f is the mass fraction of gas ingested into the probe.

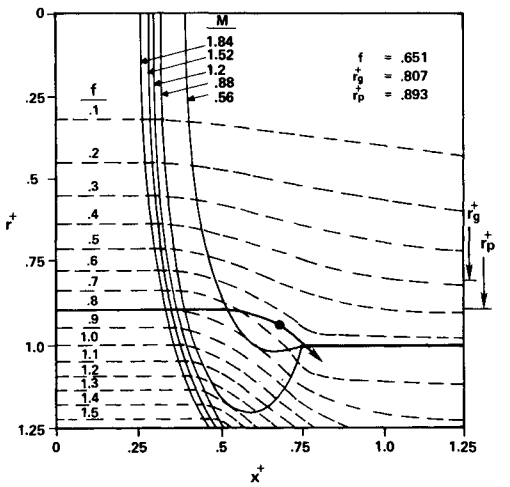

Fig. 3 Limiting particle trajectory in gas flowfield; $M=2$, $\gamma=1.4$, $\alpha=0.9$, $Kn_{01}=0.1$, $\Psi_{01}=0.15$.

desktop IBM PC AT computer with an 80287 math coprocessor. In the present study, it was assumed for simplicity that the concentration of particles is low or that the presence of particles in the gas flowfield did not affect the shock wave structure or any of the characteristics of the gas flowfield.

III. Particle Trajectories

A. Equation of Motion

The equation of motion or Newton's law was written for a rigid spherical particle moving relative to the gas in the form[3]

$$m_p \frac{dv}{dt} = -\frac{\rho}{2} A_p C_D |v - v_f| (v - v_f) \tag{1}$$

Here, m_p is the particle mass, ρ the fluid density, C_D the drag coefficient, A_p the particle cross-sectional area, and v and v_f the particle and gas velocity, respectively. The drag coefficient $C_D(Re,Kn)$ depends on the local values of the particle Knudsen and Reynolds numbers. In the present study, a useful expression for the drag coefficient developed by Crowe[4] has been used that correlates drag data in supersonic flows and reduces to Stokes law and free molecular results in limiting case.

Dividing the equation of motion by the particle mass m_p, the initial particle and gas velocity v_1, and the probe radius $R = D/2$, one obtains the four coupled nonlinear ordinary differential equations

$$\frac{du^+}{d\theta} = \frac{-C_D(Kn,Re)}{24}\left(\frac{Rep}{\Psi}\right)|v^+ - v_f^+|(u^+ - u_f^+) \tag{2}$$

$$\frac{dv^+}{d\theta} = \frac{-C_D(Kn,Re)}{24}\left(\frac{Rep}{\Psi}\right)|v^+ - v_f^+|(v^+ - v_f^+) \tag{3}$$

$$\frac{dx^+}{d\theta} = u^+ \tag{4}$$

$$\frac{dr^+}{d\theta} = v^+ \tag{5}$$

subject to the boundary conditions $\theta = 0$, $u^+ = u_f^+ = 1$, $v^+ = v_f^+ = 0$, $x^+ = 0$, and $r^+ = r_p^+$. Here, $\theta = v_1 t/R$ is the normalized time and $v^+ = v/v_1$, $r_p^+ = r_p/R$ are the normalized velocity and starting coordinates of the particle, respectively. In Eqs. (2-5), x and r refer to the axial and radial coordinates while u and v refer to the axial and radial velocities.

The particle Stokes number Ψ that appears in Eqs. (2) and (3) is defined as

$$\Psi = \rho_p d_p^2 v_1 / 18\mu R \tag{6}$$

where ρ_p is the particle density, d_p the particle diameter, and R the probe radius. The particle Reynolds number based on the freestream velocity appearing in Eqs. (2) and (3) is

$$Rep = \rho d_p v_1 / \mu \tag{7}$$

or the local particle Reynolds number can be written in the form

$$Re = Rep\,|v^+ - v_f^+| \tag{8}$$

The remaining dimensionless group that appears in the equations of motion is the particle Knudsen number defined as

$$Kn = (\pi\gamma/2)^{1/2}(\mu/c\rho d_p) \tag{9}$$

where γ is the ratio of specific heats for the gas and $c = (\gamma R_g T)^{1/2}$ is the local speed of sound.

B. Numerical Methods

Equations (2-5) were solved numerically with Ralston's second-order method. A step size of $\Delta\theta = 0.01$ for the independent variable was found to be sufficient for three-place accuracy in the particle trajectory. Local values of the gas properties were determined by averaging over the four nearest grid points for each step forward $\Delta\theta$.

A particle trajectory was determined by choosing a particle Knudsen and Stokes number based on stagnation conditions upstream of the probe shock for each matrix of gas properties. The starting coordinate was subsequently adjusted until the limiting trajectory of the particle was found which intersected the probe tip. New guesses for the particle starting coordinate were made after each run with the secant method until the particle starting position r_p^+ for a limiting trajectory was determined to three decimal places.

An example of a particle limiting trajectory is shown in the flowfield of Fig. 3, where $f = 0.651$ represents the mass fraction of gas ingested into the probe. The indicated gas ingestion rate of Fig. 3 was determined numerically in earlier calculations[2] by imposing a ratio of static-to-stagnation pressure inside the probe $\alpha = 0.9$ and assuming a freestream Mach number $M = 2.0$. In Fig. 3, the solid lines are the contours of a contant Mach number while the dashed lines are streamlines. The normalized parameters r_g^+ and r_p^+ refer to the limiting gas and particle streamlines as will be defined in the following section.

C. Collection Efficiency

The collection efficiency of the particle probe E is defined for a given particle size as the ratio of particles ingested to those incident on the probe cross-sectional area. Thus, one obtains

$$E = r_p^{+2}$$

where r_p^+ is the normalized radial starting coordinate of the limiting trajectory for a given stagnation Stokes and Knudsen number. Similarly, the mass fraction of gas ingested into the probe f is defined such that

$$f = r_g^{+2}$$

where r_g^+ is the normalized radial starting coordinate of the limiting gas streamline. Since $r_p^+ \to r_g^+$ or $E \to f$ in the limit as the particle Stokes number $\Psi \to 0$ and $r_p^+ \to 1$ or $E \to 1$ for large Ψ, it is convenient to define a reduced particle collection efficiency E_p such that

$$E_p = (E - f)/(1 - f) \tag{10}$$

where $0 \le E_p \le 1$.

IV. Similitude

A. Knudsen Number

The particle Stokes number defined by Eq. (6) represents the ratio of the particle stopping distance to the probe radius. The stopping distance is computed assuming the linear Stokes drag law (small-particle Reynolds number) for a particle initially moving with the freestream velocity. If the Knudsen number of the particle is large, departures from the continuum flow are accounted for by including the Cunningham slip correction factor[5-7]:

$$\Phi_c = 1 + 2Kn(1.257 + 0.4e^{-0.55/Kn}) \tag{11}$$

in the linear drag law such that particle collection efficiency is now scaled by an impaction parameter of the form

$$\Psi_c = \Psi\Phi_c(Kn) \tag{12}$$

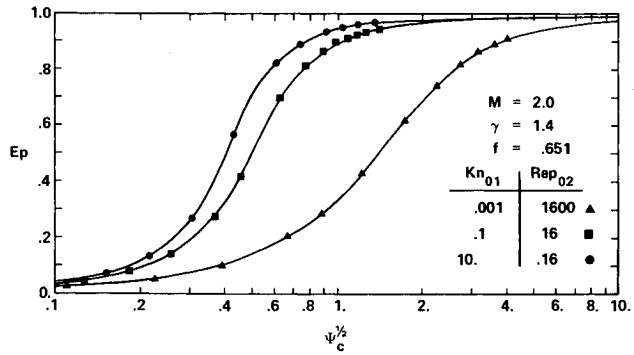

Fig. 4 Reduced collection efficiency indicating effect of large-particle Reynolds number.

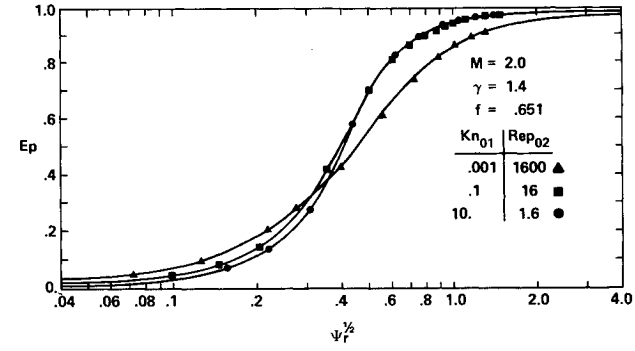

Fig. 5 Reduced collection efficiency corrected for large-particle Reynolds number.

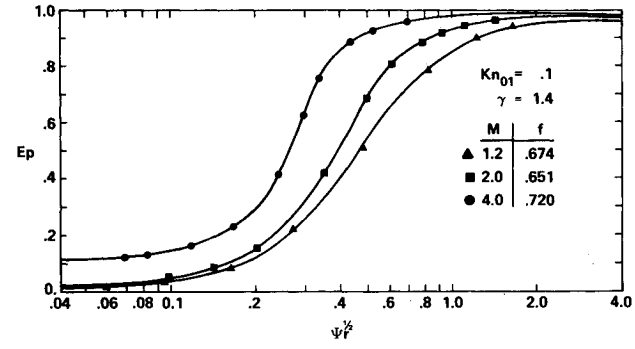

Fig. 6 Reduced collection efficiency indicating effect of freestream Mach number.

For supersonic flows where particle relaxation occurs downstream of a detached shock, it is appropriate to compute the particle Knudsen, Stokes, and Reynolds numbers in terms of stagnation conditions downstream of the shock. Thus, in Fig. 4, numerical results for the reduced collection efficiency E_p are plotted as a function of the parameter $\psi_c^{1/2}$ where

$$\Psi_c = \Psi_{02}\Phi_c(Kn_{02}) \tag{13}$$

Here,

$$\Psi_{02} = \Psi_{01}, \qquad \Psi_{01} = \rho_p d_p^2 v_1 / 18\mu_{01} R$$

and

$$Kn_{02} \approx Kn_{01}(\rho_{01}/\rho_{02})$$

where ρ_{01}, ρ_{02} are the stagnation gas densities upstream and downstream of the shock, respectively.[3]

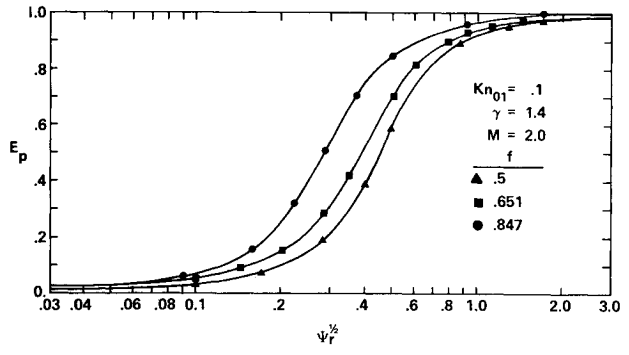

Fig. 7 Reduced collection efficiency indicating effect of probe ingestion rate.

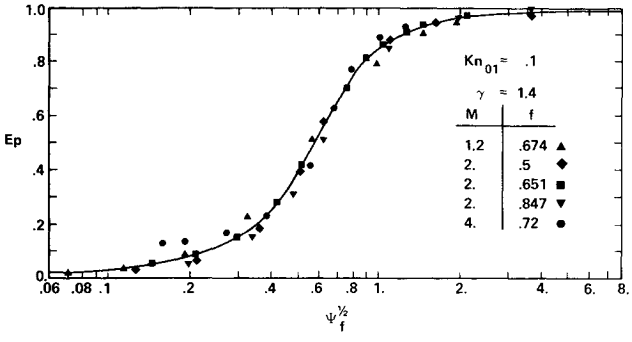

Fig. 8 Reduced collection efficiency vs the particle impaction parameter. Solid symbols represent numerical results.

It is apparent, however, that the use of Ψ_c in Fig. 4 is not adequate to correlate the numerical computations of the reduced particle collection efficiency. Clearly, the use of the Stokesian drag law in the numerical computations leading to Fig. 4 is inadequate because of the effects of large-particle Reynolds numbers.

B. Reynolds Number

The gas velocities in supersonic streams are large, and this leads to large particle Reynolds numbers downstream of the shock. For example, a stagnation Knudsen number upstream from the shock $Kn_{01} = 0.1$ corresponds roughly to a particle diameter $d_p \sim 0.1$ μm at standard conditions. One notes from Fig. 4, however, that the Reynolds number downstream of the shock at $M = 2$ is $Rep_{02} = 16$, or that the drag law for a $d_p \sim 0.1$ μm particle is non-Stokesian.

Recently, Israel and Rosner[8] included the effects of non-Stokesian drag in the derivation of the particle stopping distance for subsonic flows ($M \leq 0.4$) and thus obtained a generalized impaction parameter or Stokes number defined as follows:

$$\Psi_r = \frac{4}{3}\left(\frac{\rho_p}{\rho}\right)\left(\frac{d_p}{R}\right)\Phi_c \int_0^{Rep} \frac{dRe}{C_D Re} \tag{14}$$

The inertial effects included in the derivation of Eq. (14) refer to the influence of a larger-particle Reynolds number on the particle drag coefficient, as will be shown. However, Eq. (14) neglects the virtual mass term in the particle drag law.

In the adaptation of Eq. (14) to the present problem, the dependence of the drag coefficient on the particle Reynolds number for a large Re is approximated by[7]

$$C_D = (24/Re)(1 + 0.158Re^{2/3}) \tag{15}$$

Integrating Eqs. (14) and (15) such that $Rep = Rep_{02}$, one obtains

$$\Psi_r = \Psi_{01}\Phi_c(Kn_{02})\Phi_r(Rep_{02}) \tag{16}$$

where

$$\Phi_r(Rep_{02}) = \frac{18}{Rep_{02}}\left[Rep_{02}^{1/2} - 2.52\,\tan^{-1}\left(\frac{Rep_{02}^{1/2}}{2.52}\right)\right] \tag{17}$$

$$Rep_{02} = Rep_{01}(\rho_{02}/\rho_{01}) \tag{18}$$

Here, changes in the gas viscosity μ in Eq. (18) can be neglected since the stagnation temperature remains unchanged across the probe shock.[3] Moreover,

$$Rep_{01} = \rho_{01} v_1 d_p/\mu_{01} \tag{19}$$

where it is possible to show that[3]

$$Rep_{01} = \left(\frac{\pi\gamma}{2}\right)^{1/2}\left(\frac{1}{Kn_{01}}\right)\left[\frac{M^2}{1+[(\gamma-1)/2]M^2}\right]^{1/2} \tag{20}$$

The numerical data of Fig. 4 for the reduced collection efficiency E_p was replotted with Ψ_r defined in Eq. (16). Thus, one obtains a reasonable correlation of the results with a single universal function of Ψ_r as demonstrated in Fig. 5. Some departure is noted from a universal curve in the upper and lower segments of the sigmoidal plots because of the difference between the drag coefficient of Crowe[4] introduced into the equations of motion (2) and (3) and the simple form for C_D suggested by Eq. (15).

C. Shock Detachment Distance

Particle impaction from subsonic incompressible flows is correlated with the knowledge of two characteristic lengths: the collector dimension and particle stopping distance. If the collector is suspended in a supersonic stream, the shock detachment distance, which depends on the collector geometry, freestream Mach number, and, in the present problem, the gas ingestion rate will strongly influence the collection efficiency.[2,9]

From the experimental data for the shock detachment distance on a solid cylinder aligned parallel to the freestream,[10] one obtains an empirical expression

$$\left(\frac{\delta}{R}\right)_{f=0} = \frac{1.78}{M}[1 - 0.46(M-2) + 0.32(M-2)^2] \tag{21}$$

where δ is the detachment distance. Moreover, from our previous numerical work,[2] the effect of the probe ingestion rate f on the shock detachment distance at a freestream Mach number $M=2$ can be predicted to within 5% with the expression

$$\frac{\delta}{R} = \left(\frac{\delta}{R}\right)_{f=0}\cos\left(\frac{f\pi}{2}\right), \quad 0 \le f \le 1 \tag{22}$$

Thus, Eq. (22) with $(\delta/R)_{f=0}$ substituted from Eq. (21) provides a reasonable prediction of the shock detachment distance for the present study.

D. Effective Stokes Number

The effect of the gas freestream Mach number on the reduced probe collection efficiency E_p is indicated in Fig. 6 for three values of M: 1.2, 2, and 4. It is clear that the use of the impaction parameter Ψ_r defined by Eq. (16) does not properly account for changes in the freestream Mach number. Likewise, numerical predictions of the reduced collection efficiency E_p are strongly affected by changes in the probe ingestion rate f shown in Fig. 7.

To account for the effects indicated in Figs. 6 and 7, the impaction parameter Ψ_r is rescaled in terms of the shock detachment distance δ, which depends on both M and f. Since $\Psi_r \propto 1/R$, one obtains a correction factor of the form

$$\Phi_s(M,f,\gamma) = R/\delta \tag{23}$$

where R/δ is given by Eq. (22). Therefore, the effective Stokes number Ψ_f representing the ratio of particle stopping-to-shock detachment distance, where the former length accounts for both particle slip flow and inertial effects, becomes

$$\Psi_f = \Psi_{01}\Phi_c(Kn_{02})\Phi_r(Rep_{02})\Phi_s(M,f,\gamma) \tag{24}$$

The numerical data for the reduced collection efficiency E_p of Figs. 6 and 7 are replotted with Ψ_f. These results are correlated with a single universal curve, as indicated in Fig. 8. Thus, particles smaller than a critical size d_p^* defined by the expression

$$E_p(\sqrt{\Psi_f^*}) = 0.5 \tag{25}$$

are not subject to discrimination at the probe inlet where $\Psi_f^* = 0.33 \pm 0.03$. Moreover, the impaction parameter Ψ_f should have utility in attempts to predict the particle impaction on a variety of shapes suspended in supersonic streams.

Acknowledgment

The present study was sponsored by Sverdrup Technology Inc., Arnold AFS, TN, under Subcontracts A-84-EL-024, A5S-081, and A65-037.

References

[1]Forney, L. J., McGregor, W. K., and Girata, P. T., "Particle Sampling with Supersonic Probes: Similitude and Particle Breakup," AEDC-TR-83-26, Arnold AFS, TN, 1983.

[2]Forney, L. J., McGregor, W. K., and Van Dyke, D. B., "Computation of Gas Flowfields in Supersonic Particle Probes," *ASME Journal of Fluids Engineering*, Vol. 76, March 1986, pp. 76-81.

[3]Forney, L. J., McGregor, W. K., and Van Dyke, D. B., "Dynamics of Particle-Shock Interactions, Part I: Similitude," *Aerosol Science and Technology*, Vol. 6, April 1987, pp. 129-141.

[4]Crowe, C. T., "Drag Coefficient of Particles in a Rocket Nozzle," *AIAA Journal*, Vol. 5, May 1967, pp. 1021-1022.

[5]Forney, L. J. and McGregor, W. K., "Scaling Laws for Particle Breakup in Nozzle Generated Shocks," *Particulate Science and Technology*, Vol. 1, 1983, pp. 419-431.

[6]Forney, L. J., Walker, A. E., and McGregor, W. K., "Dynamics of Particle-Shock Interactions, Part II: Effect of the Basset Term," *Aerosol Science and Technology*, Vol. 6, April 1987, pp. 143-152.

[7]Friedlander, S. K., *Smoke Dust and Haze: Fundamentals of Aerosol Behavior*, John Wiley, New York, 1976.

[8]Israel, R. and Rosner, D. E., "Use of a Generalized Stokes Number to Determine the Aerodynamic Capture Efficiency of Non-Stokesian Particles from a Compressible Gas Flow," *Aerosol Science and Technology*, Vol. 2, Jan. 1983, pp. 45-51.

[9]Martone, J. A., Daley, P. S., and Boubel, R. W., "Sampling Submicrometer Particles Suspended in Near Sonic and Supersonic Free Jets," *Journal of the Air Pollution Control Association*, Vol. 30, Aug. 1980, pp. 898-903.

[10]Leipmann, H. W. and Roshko, A., *Elements of Gas Dynamics*, John Wiley, New York, 1957.